Domain Structures in Epitaxial $(10\bar{1}0)$ Co Wires

I. L. Prejbeanu, L. D. Buda, U. Ebels, M. Viret, C. Fermon, and K. Ounadjela

Abstract—A systematic investigation of the magnetic domain structure is presented for epitaxial sub-micron $(10\bar{1}0)$ Co wires characterized by a strong in-plane uniaxial magneto-crystalline anisotropy whose easy axis is oriented perpendicular to the long wire axis. Wires of varying width (100 to 1000 nm) and thickness (30 to 80 nm) were patterned by electron beam lithography and lift-off process. We establish experimentally the boundaries between the ground state transverse single domain state and the open stripe structure as a function of wire thickness and width. Moreover, the stability of the transverse single domain state is investigated as a function of the magnetization history.

Index Terms—MFM, micromagnetics, stripe domains.

I. INTRODUCTION

THE OBSERVATION of a domain wall magnetoresistance effect in magnetic wires exhibiting either a stripe domain structure [1]–[3] or longitudinal single domains with head-to-head domain walls [4], [5] has revealed the possible role of spin dependent scattering and spin accumulation for the spin dependent transport through domain walls. In this interpretation, the internal structure of the domain wall and the evolution of the domain structure in an applied field play a crucial role to separate other MR effects from the domain wall resistance effect. A number of these transport experiments were performed on hcp Co wires [1], [2], [4] which are characterized by a relatively strong uniaxial magneto-crystalline anisotropy, $K_u = 5 - 6 \times 10^6$ erg/cm^3, yielding a moderate Q-factor of 0.4 ($Q = K_u/(2\pi M_s^2)$, M_s = saturation magnetization). Besides the interest of such sub-micron Co wires for the study of magneto-transport properties, the moderate Q-factor makes the system interesting as well to investigate the stability range of different micromagnetic configurations in confined geometries of submicron scale. In this paper, flat rectangular Co wires are investigated, for which the uniaxial magneto-crystalline anisotropy is in-plane and perpendicular to the wire axis. In this case, the competition between the magneto-crystalline anisotropy, the shape anisotropy and the exchange energy induces stripe domains. The stability of these stripe domains is investigated as a function of the magnetic history. The boundary between the transverse single domain state and the open stripe domain state is established as a function of the wire thickness t and of the wire width w.

II. EXPERIMENTAL PROCEDURE

The wires were prepared from epitaxial $(10\bar{1}0)$ Co thin films of thickness $t = 30, 40, 50, 60$, and 80 nm. The films were grown under ultrahigh vacuum conditions on (110) MgO substrates by molecular beam epitaxy using a Mo-Cr buffer layer. Structural investigations confirm the hcp structure and magnetic investigations confirm a strong in-plane uniaxial anisotropy [6]. The films were patterned using electron-beam lithography, lift-off techniques and ion beam etching. For each thickness, wire arrays were prepared for wire widths of $w = 100, 150, 200, 500, 800$ and 1000 nm. The wires are 10 μm long and the separation between the wires is 5 μm, sufficient to neglect any dipolar interaction. For each set of (t, w)-values, wires were patterned whose long wire axis is aligned perpendicular to the magneto-crystalline anisotropy axis. The magnetic microstructure was investigated by magnetic force microscopy (MFM) in the phase-detection mode (Digital Instruments, Nanoscope 3100). Commercial CoCr coated Si cantilevers of pyramidal shape, magnetized along the tip axis, were used to image the domain structures at a lift scan height of 100 nm.

III. RESULTS AND DISCUSSION

The competition between the magneto-crystalline anisotropy and the shape anisotropy induces a stripe domain structure, similar to the continuous bubble-type films for which the magneto-crystalline easy axis is perpendicular to the film plane [7], [8]. In a further analogy, the periodicity of the stripe domains depends sensitively on the wire width and thickness, but also on the magnetic history. The latter is demonstrated in Fig. 1(a) by the MFM images taken for the same wire at zero field after different magnetization histories. Here, R denotes a remanent state and D a demagnetized state. Furthermore, $R \parallel K_u$ and $D \parallel K_u$ denote the application of the field in-plane and parallel to the magneto-crystalline easy axis (perpendicular to the long wires axis), $R \parallel s$ and $D \parallel s$ denote the application of the field in-plane and along the magneto-crystalline hard axis ($\mathbf{s}$ = easy shape anisotropy axis, parallel to the long wire axis) and $R\perp$ and $D\perp$ denote the application of the field out of plane.

For the 60 nm thick and 800 nm wide wire shown in Fig. 1(a), the easy axis procedures $R \parallel K_u$ and $D \parallel K_u$ induce a transverse single domain state, while any hard axis magnetization procedure $(R \parallel s, D \parallel s, R\perp, D\perp)$, induces a stripe domain structure. The single domain states $R \parallel K_u$ and $D \parallel K_u$ are metastable states. Applying the field parallel to the easy magneto-crystalline anisotropy axis gives a preferential orientation to the magnetization $\mathbf{M}$, blocking $\mathbf{M}$ in a local energy minimum, which is separated by an energy barrier from the
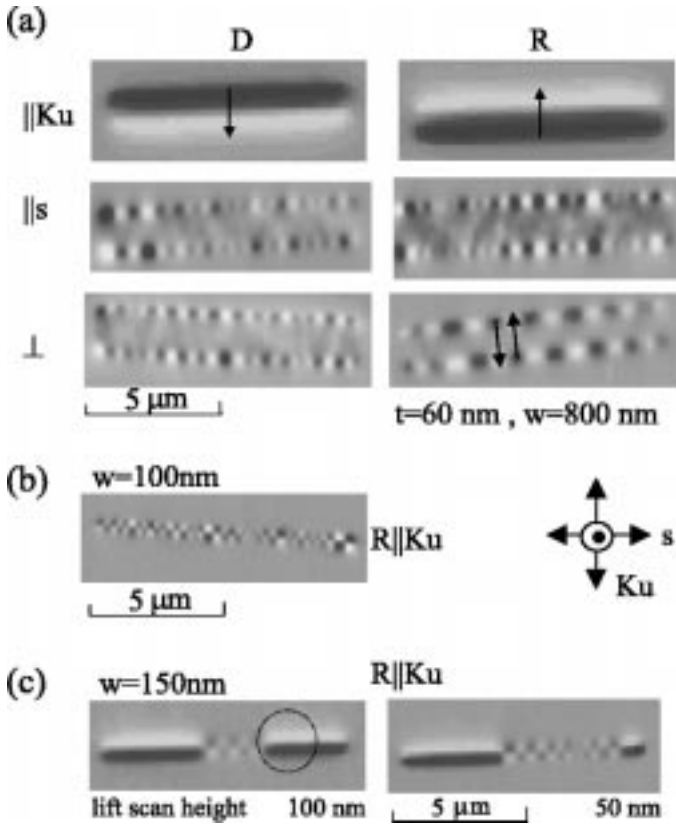
Fig. 1. (a) MFM images for a $t = 60$ nm and $w = 800$ nm wire after different magnetization histories as explained in the text and as indicated on top and at the left of the images. The arrows indicate the magnetization orientation. (b) MFM image of a $t = 60$ nm and $w = 100$ nm wire after in-plane easy axis saturation $R \parallel K_u$. (c) MFM images of a $t = 60$ nm and $w = 150$ nm wire after in-plane easy axis saturation $R \parallel K_u$, scanned at two different lift scan heights, as indicated below the images. The dotted circle shows the region where the stripe domain structure is induced by the tip.

Fig. 2. (a) The experimental domain width L as a function of w for $t = 60$ nm and for different magnetization histories. (b) and (c) are schematics indicating the magnetization fluctuation below the saturation field for the saturation procedure $R \parallel s$ (b) and $R\perp$ (c). In (c) only the projection of the magnetization into the wire plane is shown.

multi-domain stripe state. This barrier decreases, the narrower and the thicker the wires, due to the increase in the in-plane shape demagnetization fields which favor the nucleation of reverse domains. This is confirmed in Fig. 1(b) showing stripe domains after easy axis magnetization $R \parallel K_u$ in a much narrower wire ($w = 100$ nm). Local defects along the edges also can reduce the barrier and induce a stripe domain state during the magnetization process. Furthermore, a perturbation of the metastable single domain state at zero field can be induced by the MFM tip. As shown in the left MFM image of Fig. 1(c), the single domain and the stripe domain state coexist for a narrow wire of $w = 150$ nm after easy-axis magnetization, $R \parallel K_u$. A small perturbation arising from the stray fields of the MFM tip produces in some regions an irreversible transition into the stripe domain state [9]. The tip stray field felt by the wire was increased in the left image of Fig. 1(c) by lowering the lift scan height from 100 nm to 50 nm. Using the easy-axis magnetization or demagnetization processes, a boundary in the (t, w)-plane can be defined, separating a metastable single domain state at large w and low t, from a stripe domain state, at low w and large t. For the stripe domain state, one also has to distinguish between a stable and a metastable configuration. The stripe domain state, induced by the easy axis processes $R \parallel K_u, D \parallel K_u$ is not a ground state. The domain sizes are much larger than
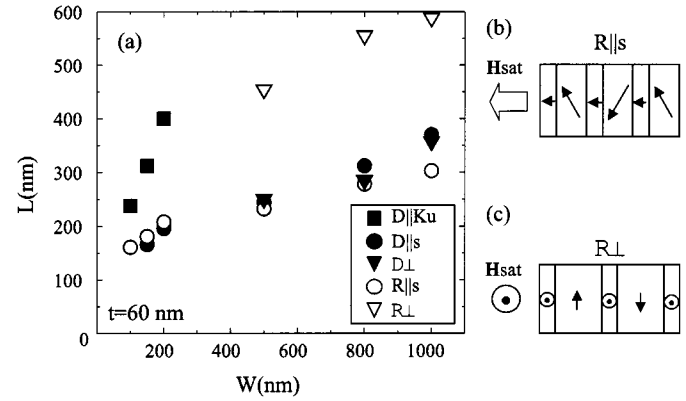
those obtained after hard axis magnetization or demagnetization ($R \parallel s, D \parallel s, R\perp, D\perp$).

In Fig. 2(a) the domain size L as a function of wire width w is summarized for $t = 60$ nm using five different magnetization histories. Clearly, L is much larger for the easy axis demagnetization $D \parallel K_u$ (full squares) than for the hard axis demagnetization procedures $D \parallel s$ (full circles) and $D\perp$ (full triangles), which yield the same value for L. Furthermore, it is interesting to note that the out of plane remanent state $R\perp$ (open triangles) yields domain widths L which are almost twice as large as those obtained for the in-plane hard axis remanent state $R \parallel s$ (open circles), whose domain width L is comparable to the hard axis demagnetization procedures $D \parallel s$ and $D\perp$, see also the corresponding MFM images in Fig. 1(a). This difference can be explained by thenucleation procedure of the stripes. At the onset of nucleation, just below saturation, the magnetization starts to rotate away from the field direction toward the magneto-crystalline easy axis. In order to reduce the arising in-plane demagnetization field energy a continuous magnetization fluctuation with an alternating in-plane magnetization component ($\parallel K_u$) develops, see Fig. 2(b), (c). Below the in-plane hard axis saturation $R \parallel s$, the domains of opposite in-plane magnetization component are separated by low-angle Néel-type walls (Fig. 2(b)), which contain weak dipolar charges. In contrast, for the out of plane magnetization $R\perp$, just below saturation, low-angle Bloch-type walls arise inside which the spins remain perpendicular to the film surface (Fig. 2(c)). To minimize the strong out-of-plane demagnetization field energy of these wall spins, the number of initial walls created below the $R\perp$ saturation is reduced, resulting in larger domain sizes. In conclusion, the best procedure to relax the system into its ground state without having to overcome additional energy barriers, is the in-plane hard axis saturation or demagnetization $R \parallel s$ and $D \parallel s$.

Having established the transition between the metastable transverse single domain state and the stripe domain state, we now turn to the transition between these two configurations as stable ground state configurations. The stable ground states were obtained from the hard axis demagnetization procedures and typical MFM images are shown in the inset (a) of Fig. 3 as a function of t for $w = 800$ nm. For decreasing film thickness
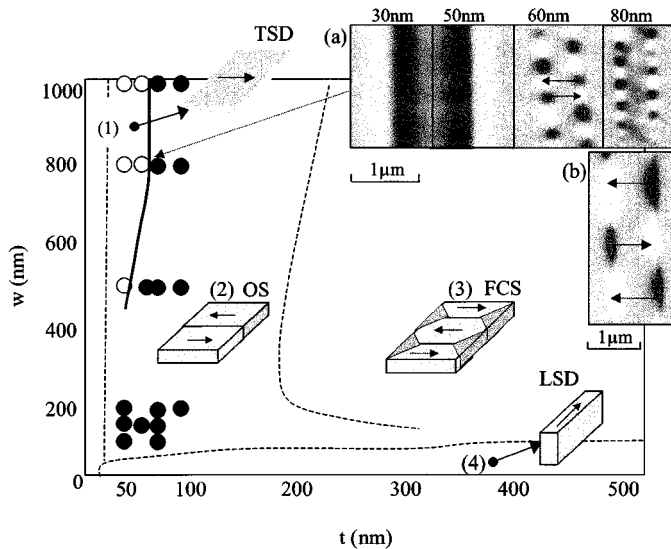
Fig. 3. The (w, t)-diagram of the ground state domain configuration. The bold line is the experimental boundary between the single domain (open circles) and stripe domain state (full circles). The dotted lines are calculated boundaries. (a) MFM images for wires of $w = 800$ nm and t as indicated. (b) Zoom of an MFM image, showing in detail the dipolar contrast of the open stripe structure.

and increasing wire width, the gain in demagnetization energy by nucleating the stripe domain state decreases. For some critical values the gain will not be sufficient to compensate the wall energy. Hence the system acquires a (transverse) single domain state. The bold line in the (w, t)-diagram of Fig. 3 summarizes the experimental boundary between the stable stripe domain state (full circle) and the stable transverse single domain (open dot) state. This is in approximate agreement with the boundary calculated (dotted lines) from a domain theory model based on Kittel's formulation [10]. For the calculation, four different domain configurations were considered: (1) the longitudinal single domain state (LSD), with $\mathbf{M}$ parallel to the wire axis (2) the transverse single domain state (TSD) with $\mathbf{M}$ perpendicular to the wire axis, (3) an open stripe structure (OS) and (4) a stripe domain structure with flux closure domains (FCS). The phase boundaries were obtained by comparing the total energy density for all four configurations and choosing the configuration of lowest energy. The demagnetization energy was calculated, from a 'charged sheet' model, by which only charges at the long side faces are taken into account [11].

A constant wall energy density (12 erg/cm^2) was used which explains the shift between the calculated and the experimental boundary separating the TSD and the OS states. Since the wall energy is not known exactly, a value close to the bulk value was chosen. In reality this value maybe much larger, due to the vertical and lateral confinement [11]. In order to obtain a better estimate, the wall structure itself needs to be known. Preliminary 3D micromagnetic calculations [12] indicate that a wall can be stabilized having a structure similar to the complete flux closure domains FCS shown in the diagram of Fig. 3. The FCS, however, is narrower so that a substantial opening between the walls would remain.

This may raise the question whether the stripe domain structure observed in the experiment is of the OS or the FCS type. A zoom of the MFM contrast is shown in the inset (b) of Fig. 2.

The regions of strong contrast have an elliptical shape, with a reduced contrast at the transition from black to white. This pattern is quite different from the one obtained in [1] for the complete FCS of low-Q Fe(110) wires ($w = 2 \ \mu$m, $t = 50$ nm, $Q = 2.5 \ 10^{-2}$). In this case, the contrast is very strong in the transition region from black to white, due to the volume charges of the flux closure domains. From this comparison it is concluded that the contrast observed here in the Co($10\bar{1}0$) wires corresponds to the open stripe structure. The exact structure of the domain walls however remains an issue to be addressed in further experiments. So far no wall contrast was observed, since the images are dominated by the strong dipolar contrast of the open domains.

IV. CONCLUSION

In conclusion, the stable and metastable magnetization configuration for Co($10\bar{1}0$) submicron wires have been investigated by MFM using different magnetization histories. The phase boundary between the stable open stripe domain structure and the transverse single domain structure were established which is in agreement with the boundary calculated from a simple domain theory model.

REFERENCES

[1] A. D. Kent, U. Rüdiger, J. Yu, L. Thomas, and S. S. P. Parkin, "Magnetoresistance, micromagnetism, and domain wall effects in epitaxial Fe and Co structures with stripe domains," *J. Appl. Phys.*, vol. 85, p. 5243, 1999.

[2] S. G. Kim, Y. Otani, K. Fukamichi, S. Yuasa, M. Nyvlt, and T. Katayama, "Magnetoresistivity of micron size epitaxial Co (10.0) wires," *IEEE Trans. Magn.*, vol. 35, p. 2862, 1999.

[3] M. Viret, Y. Samson, P. Warin, A. Marty, F. Ott, E. Søndergård, O. Klein, and C. Fermon, "Anisotropy of domain wall resistance," *Phys. Rev. Lett.*, vol. 85, p. 3962, 2000.

[4] U. Ebels, A. Radulescu, Y. Henry, L. Piraux, and K. Ounadjela, "Spin accumulation and domain wall magnetoresistance in 35 nm Co wires," *Phys. Rev. Lett.*, vol. 84, p. 983, 2000.

[5] T. Taniyama, I. Nakatani, T. Namikawa, and Y. Yamazaki, "Resistivity due to domain walls in Co zigzag wires," *Phys. Rev. Lett.*, vol. 82, p. 2780, 1999.

[6] I. L. Prejbeanu, L. D. Buda, U. Ebels, and K. Ounadjela, "Observation of asymmetric bloch walls in epitaxial Co films with strong in-plane uniaxial anisotropy," *Appl. Phys. Lett.*, vol. 77, p. 3066, 2000.

[7] C. Kooy and U. Enz, "Experiment and theoretical study of the domain configuration in thin layers of BaFe$_{12}$O$_{19}$," *Philips Res. Rep.*, vol. 15, p. 7, 1960.

[8] M. Hehn, S. Padovani, K. Ounadjela, and J.-P. Bucher, "Nanoscale magnetic domain structures in epitaxial cobalt films," *Phys. Rev. B*, vol. 54, p. 3428, 1996.

[9] For example, the stray field of the tip for a scan height of 20 nm and a pyramidal tip of 6 nm height produces an in-plane stray field of 15 Oe. Taking into account that a real tip is at least 10 times thicker, the actual field may take values up to 100 Oe.

[10] C. Kittel, "Theory of the structure of ferromagnetic domains in films and small particles," *Phys. Rev.*, vol. 70, p. 965, 1946.

[11] A. Hubert and R. Schäfer, *Magnetic Domains*, Berlin: Springer, 1998. p. 122 (demagnetization energy) and p. 251 (wall energy).

[12] L. Buda, Vortex state stability in circular Co (0001) dots, in The calculations used are summarized in thess proceedings, paper no: CE-03.